Journal of Photochemistry and Photobiology A: Chemistry 201 (2009) 128–135

Contents lists available at ScienceDirect

Journal of Photochemistry and Photobiology A: Chemistry

journal homepage: www.elsevier.com/locate/jphotochem

New NIR-emitting complexes of platinum(II) and palladium(II) with fluorinated benzoporphyrins

S.M. Borisov[a,*], G. Nuss[a], W. Haas[a], R. Saf[b], M. Schmuck[b], I. Klimant[a]

[a] Institute of Analytical Chemistry and Radiochemistry, Graz University of Technology, Stremayrgasse 16, 8010 Graz, Austria
[b] Institute for Chemistry and Technology of Materials, Graz University of Technology, Stremayrgasse 16, 8010 Graz, Austria

ARTICLE INFO

Article history:
Received 12 June 2008
Received in revised form
30 September 2008
Accepted 10 October 2008
Available online 17 October 2008

Keywords:
Benzoporphyrin
Phosphorescence
Metal complex
Oxygen quenching

ABSTRACT

New platinum(II) and palladium(II) complexes with fluorinated benzoporphyrins are prepared and characterized. The photo-physical and electrochemical properties, as well as quenching by oxygen are investigated. The complexes possess highly efficient room-temperature NIR phosphorescence and are excitable with blue- and red-light. The fluorinated derivatives show improved photo-physical properties and photo-stability. The new dyes are particularly suitable as indicators for the use in optical oxygen sensors.

1. Introduction

Determination of oxygen is of a great importance in various fields of science and technology. Optical sensing and imaging of oxygen is virtually non-invasive and thus it has become extremely popular in the last two decades [1]. UV–vis oxygen indicators are fairly established and are mainly represented by ruthenium(II) polypyridyl complexes (particularly, ruthenium(II)-tris-4,7-diphenyl-1,10-phenanthroline (Ru-dpp)) [2–5], palladium(II) and platinum(II) complexes with porphyrins [6–10], and cyclometallated complexes of platinum(II) and iridium(III) [11–13]. Optical sensors based on UV–vis indicators, however, suffer from some drawbacks. First, a high level of autofluorescence in many biological media is produced upon excitation, since many natural compounds are fluorescent. Typical examples include nucleotides FAD and NAD, which are present in many biological samples and in fermentation media. Many components of an optical set-up (such as long-pass filters or fibers) also can generate background fluorescence; therefore, long-waved excitation allows for purer optical signals. Second, UV–vis indicators are poorly suitable for measurements in scattering media. High scattering is common in bioreactors and in marine sediments, as well as in the case of measurements performed in subcutaneous tissue. Third, UV–vis indicators cannot be used in implantable sensors, since highly scattering blood components efficiently absorb in visible region. Lack of appropriate indicators is thus a serious hindrance for the development of implantable sensors for subcutaneous glucose measurements since this sensor type also relies on oxygen transduction [14].

NIR-excitable probes overcome these drawbacks, but also show much better compatibility with optical components. For example, bright LEDs and laser diodes are available as excitation sources starting from 590 to 630 nm, respectively, while the sensitivity of cheap and compact Si photo-diodes increases at longer wavelengths and reaches maximum at 850–900 nm. A few NIR indicators were reported to be suitable for oxygen sensing. The Pt(II) and Pd(II) complexes of porphyrin lactones [15] and porphyrin ketones [16] possess intense absorption bands in the region 580–600 nm and some of them are excellently compatible with a 590-nm LED. Despite relatively high absorption coefficients the complexes exhibit moderate to low brightnesses (BS, determined as the product of molar absorption coefficient, ε and emission quantum yield, Φ). Moreover, the indicators are practically unsuitable for measurements in subcutaneous tissue or blood since transmittance of the excitation-light is still rather low. The palladium(II) complexes with benzoporphyrins [17] and naphthoporphyrins [17–19] seem to be much more promising for optical sensing [20]. The benzoporphyrin complexes, particularly, possess good brightnesses [17] upon excitation in the red region ($\lambda_{max} > 600$ nm) and are nicely compatible with LEDs and laser diodes. Unfortunately, the luminescence decay time of the palladium(II) complexes often is too long (~400 μs) and the sensitivity to oxygen is too high to provide optimal dynamics in most sensor materials. The respective platinum(II) complexes

* Corresponding author. Tel.: +43 316 873 4326 fax: +43 316 873 4329.
E-mail address: sergey.borisov@tugraz.at (S.M. Borisov).

1010-6030/$ – see front matter © 2008 Elsevier B.V. All rights reserved.
doi:10.1016/j.jphotochem.2008.10.003

(having shorter decay time) are only sparsely described in the literature and are restrained to unsubstituted benzoporphyrins [21] (that suffer from low solubility and high tendency to aggregation) and water-soluble derivatives [18]. Recently application of a platinum(II) benzoporphyrin in the NIR-OLEDs was demonstrated [22]. Thus, new benzoporphyrin complexes (particularly of platinum(II)) are of much interest for developing advanced optical sensors and biosensors. Fluorinated porphyrins can additionally benefit from improved photo-stability [10]. In this contribution we report the synthesis and photo-physical properties of new platinum(II) and palladium(II) complexes with fluorinated *meso*-tetraphenyltetrabenzoporphyrins.

2. Experimental

2.1. Materials

Ethyl isocyanoacetate, 1-nitro-1-cyclohexene, 2,3-dicyano-5,6-dichlorobenzoquinone (DDQ), poly(octadecyl methacrylate) (average MW, 170,000) and polyvinylpyrrolidone K 30 were purchased from Aldrich (www.sigmaaldrich.com). The fluorinated benzaldehydes (4-fluorobenzaldehyde, 3,5-difluorobenzaldehyde, 3,4,5-trifluorobenzaldehyde and pentafluorobenzaldehyde), palladium(II) chloride, platinum(II) chloride and benzonitrile were from ABCR (www.abcr.de). Dimethylformamide, ethyldiisopropylamine, 1,8-diazabicyclo [5.4.0] undec-7-ene (DBU), benzaldehyde, ethylcellulose (46% ethoxyl content) and poly(vinyl chloride) were obtained from Fluka (www.sigmaaldrich.com). All other solvents were from Roth (www.carl-roth.de). The silica-gel 60 (0.063–0.200 mm) was from Merck (www.merck.de). Polysterene (MW. 250,000) was obtained from Fischer Scientific (www.fishersci.com). Poly(ethylene glycol terephthalate) support (Mylar®) was purchased from Goodfellow (www.goodfellow.com). Platinum(II) octaethylporphyrine (PtOEP) and platinum(II) 5,10,15,20-tetrakis-(2,3,4,5,6-pentafluorophenyl)-porphyrin (PtTFPP) were purchased from Frontier Scientific (www.frontiersci.com). Nitrogen and synthetic-air (all of 99.999% purity) were obtained from Air Liquide (www.airliquide.at). The test gas (1% of oxygen in nitrogen) was purchased from Linde (www.linde-gas.at).

2.2. Synthesis

The synthesis of 4,5,6,7-tetrahydroisoindole and *meso*-tetraphenyltetracyclohexenoporphyrin (H_2TPTHP, Fig. 1) were performed according to a literature procedure [23]. The platinum(II) complex with *meso*-tetraphenyltetrabenzoporphyrin (PtTPTBP) was further prepared according to Borek et al. [22]. The modification includes addition of 500 μL of ethyldiisopropylamine per 700 mg of *meso*-tetraphenyltetracyclohexenoporphyrin to promote the platination. The reaction was completed within 1 h. The complexes of platinum(II) with *meso*-tetra(4-fluorophenyl) tetrabenzoporphyrin (PtTPTBPF), *meso*-tetra(3,5-difluorophenyl) tetrabenzoporphyrin (PtTPTBPF_2) and *meso*-tetra(3,4,5-trifluorophenyl)tetrabenzoporphyrin (PtTPTBPF_3) were prepared in a similar manner. Oxidation of platinum(II) complex with *meso*-tetra(3,4,5-trifluorophenyl)tetracyclohexaneporphyrin (PtTPTHPF_3) was performed in chloroform (150 mL per 500 mg of the complex) at 60 °C for 4 h. Ten equivalents (923 mg) of DDQ were used. The excess of DDQ was quenched with aqueous solution of sodium sulphate and the organic phase was purified on a silica-gel column using toluene as an eluent. Then, silica-gel was soaked with the solution of the dye and dried overnight at 60 °C. The platinum(II) complex with *meso*-tetra(3,5-difluorophenyl)tetrabenzoporphyrin also was not isolated but absorbed on silica-gel after purification by chromatography.

The respective palladium(II) benzoporphyrin complexes were prepared analogously except for the metallation step. The palladium(II) complexes with *meso*-substituted tetracyclohexenoporphyrins were obtained by boiling the respective ligand with 2 equiv. of $PdCl_2$ in tetrahydrofuran (~100 mL per 1 mmol of the ligand). The reaction was completed in 5 min after addition of 1 mL of triethylamine. The solvent was removed under reduced pressure, and the product was purified by column chromatography on silica-gel using CH_2Cl_2 as an eluent. In the last step, the palladium(II) complex with *meso*-tetra(3,5-difluorophenyl)tetrabenzoporphyrin was not isolated from the solution but absorbed on silica-gel.

2.2.1. *meso*-Tetraphenyltetracyclohexenoporphyrin (H_2TPTHP)

MS (MALDI): *m*/*z* $[MH]^+$ calc. 831.4427, found 831.4415. UV–vis: (CH_2Cl_2), λ/nm (relative intensity): neutral—440 (1.00), 535 (0.089), 575 (0.043), 614 (0.036), 677 (0.018); dication—466 (1.00), 620 (0.045), 676 (0.095).

2.2.2. *meso*-Tetra(4-fluorophenyl)tetracyclohexenoporphyrin (H_2TPTHPF)

MS (MALDI): *m*/*z* $[MH]^+$ calc. 903.4050, found 903.4077. UV–vis: (CH_2Cl_2), λ/nm (relative intensity): neutral—440 (1.00), 535 (0.077), 575 (sh), 615 (0.019), 677 (0.013); dication—467 (1.00), 618 (0.044), 677 (0.081).

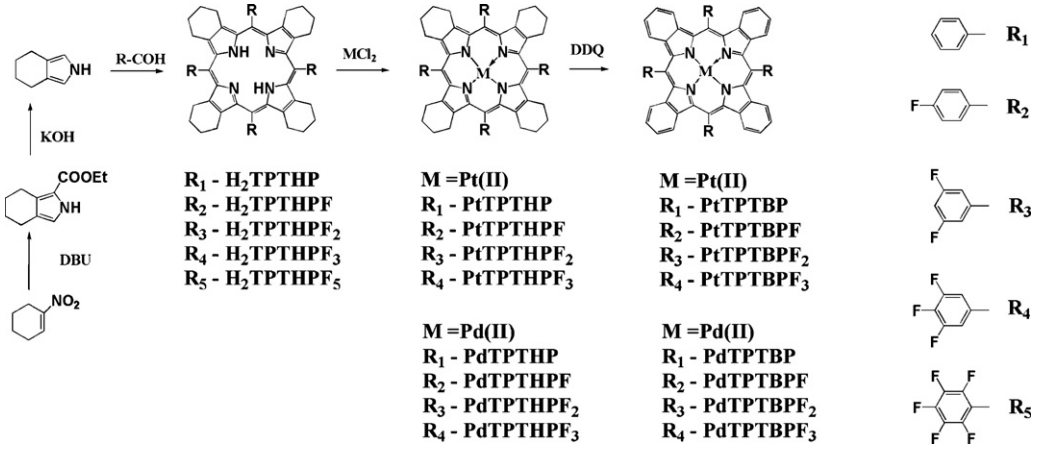

Fig. 1. Schema of synthesis and chemical structures of the benzoporphyrin complexes.

2.2.3. meso-Tetra(3,5-difluorophenyl)tetracyclohexenoporphyrin (H_2TPTHPF$_2$)

MS (MALDI): *m*/*z* [MH]$^+$ calc. 975.3673, found 975.3687. UV–vis: (CH_2Cl_2), λ/nm (relative intensity): neutral—438 (1.00), 535 (0.079), 573 (sh), 616 (0.017), 677 (sh); dication—469 (1.00), 617 (0.041), 674 (0.070).

2.2.4. meso-Tetra(3,4,5-trifluorophenyl)tetracyclohexenoporphyrin (H_2TPTHPF$_3$)

MS (MALDI): *m*/*z* [MH]$^+$ calc. 1047.330, found 1047.336. UV–vis: (CH_2Cl_2), λ/nm (relative intensity): neutral—439 (1.00), 535 (0.096), 575 (sh), 614 (0.031), 677 (sh); dication—469 (1.00), 615 (0.044), 674 (0.063).

2.2.5. Palladium (II) meso-tetraphenyltetracyclohexenoporphyrin (PdTPTHP)

MS (MALDI): *m*/*z* [M]$^+$ calc. 932.3234, found 932.3187. UV–vis: (CH_2Cl_2), λ/nm (relative intensity): 425 (1.00), 538 (0.102), 573 (0.077).

2.2.6. Palladium (II) meso-tetra(4-fluorophenyl)tetracyclohexenoporphyrin (PdTPTHPF)

MS (MALDI): *m*/*z* [M]$^+$ calc. 1004.286, found 1004.289. UV–vis: (CH_2Cl_2), λ/nm (ε/M^{-1} cm^{-1}): 426 (234000), 538 (22000), 571 (19500).

2.2.7. Palladium (II) meso-tetra(3,5-difluorophenyl)tetracyclohexenoporphyrin ($PdTPTHPF_2$)

MS (MALDI): *m*/*z* [M]$^+$ calc. 1076.248, found 1076.247. UV–vis: (CH_2Cl_2), λ/nm (relative intensity): 423 (1.00), 538 (0.093), 573 (0.104).

2.2.8. Palladium (II) meso-tetra(3,4,5-trifluorophenyl)tetracyclohexenoporphyrin ($PdTPTHPF_3$)

MS (MALDI): *m*/*z* [M]$^+$ calc. 1148.210, found 1148.218. UV–vis: (CH_2Cl_2), λ/nm (relative intensity): 423 (1.00), 538 (0.099), 573 (0.117).

2.2.9. Platinum (II) meso-tetraphenyltetracyclohexenoporphyrin (PtTPTHP)

MS (MALDI): *m*/*z* [M]$^+$ calc. 1022.382, found 1022.385. UV–vis: (CH_2Cl_2), λ/nm (relative intensity): 411 (1.00), 524 (0.068), 557 (0.077).

2.2.10. Platinum (II) meso-tetra(4-fluorophenyl)tetracyclohexaneporphyrin (PtTPTHPF)

MS (MALDI): *m*/*z* [M]$^+$ calc. 1094.344, found 1094.342. UV–vis: (CH_2Cl_2), λ/nm (ε/M^{-1} cm^{-1}): 411 (245000), 525 (18800), 558 (24400).

2.2.11. Platinum (II) meso-tetra(3,5-difluorophenyl)tetracyclohexenoporphyrin ($PtTPTHPF_2$)

MS (MALDI): *m*/*z* [M]$^+$ calc. 1166.307, found 1166.307. UV–vis: (CH_2Cl_2), λ/nm (relative intensity): 409 (1.00), 526 (0.056), 559 (0.102).

2.2.12. Platinum (II) meso-tetra(3,4,5-trifluorophenyl)tetracyclohexenoporphyrin ($PtTPTHPF_3$)

MS (MALDI): *m*/*z* [M]$^+$ calc. 1238.269, found 1238.273. UV–vis: (CH_2Cl_2), λ/nm (relative intensity): 409 (1.00), 526 (0.057), 559 (0.115).

2.2.13. Palladium (II) meso-tetraphenyltetrabenzoporphyrin (PdTPTBP)

MS (MALDI): *m*/*z* [M]$^+$ calc. 916.1982, found 916.2024.

2.2.14. Palladium (II) meso-tetra(4-fluorophenyl)tetrabenzoporphyrin (PdTPTBPF)

MS (MALDI): *m*/*z* [M]$^+$ calc. 988.1605, found 988.1567.

2.2.15. Platinum(II) meso-tetraphenyltetrabenzoporphyrin (PtTPTBP)

MS (MALDI): *m*/*z* [M]$^+$ calc. 1006.257, found 1006.257.

2.2.16. Platinum (II) meso-tetra(4-fluorophenyl)tetrabenzoporphyrin (PtTPTBPF)

MS (MALDI): *m*/*z* [M]$^+$ calc. 1078.219, found 1078.216.

2.3. Preparation of polymer films

The "cocktails" were prepared by dissolving an indicator and a polymer in an appropriate solvent (10% (w/w) of a polymer in the solvent). Chloroform was used for polystyrene and poly(vinylpyrrolidone), toluene for poly(octadecyl methacrylate), and the mixture of toluene and ethanol (80:20%, w/w) for ethylcellulose. The "cocktails" were knife-coated on a transparent polyester support to result in ~8 μm sensor films after solvent evaporation. The films contained ~0.75% (w/w) of a dye in the polymer.

2.4. Measurements

Mass Spectrometry was performed on a Micromass TofSpec 2E Time-of-Flight Mass Spectrometer. The instrument is equipped with a nitrogen laser (337 nm wavelength, operated at a frequency of 5 Hz), and a time lag focusing unit. Ions were generated by irradiation just above the threshold laser power. Positive ion spectra were recorded in reflectron mode applying an accelerating voltage of 20 kV and externally calibrated with a suitable mixture of poly(ethyleneglycol)s (PEG). The spectra of 100–150 shots were averaged to improve the signal-to-noise ratio. Analysis of data was done with MassLynx-Software V3.5 (Micromass/Waters, Manchester, UK). Samples were dissolved in THF (C = 0.1 mg mL^{-1}), dithranol was used as matrix (C = 10 mg mL^{-1} in THF). The solutions were mixed in the cap of a microtube in the ratio of 1 μL: 10 μL. Then, 0.5 μL of the resulting mixture were deposited on the sample plate (stainless steel) and allowed to dry under air.

Absorption spectra were measured at a Cary 50 UV–vis spectrophotometer (www.lzs-concept.com). Emission spectra were acquired on a Hitachi F-7000 fluorescence spectrometer (www.inula.at) equipped with a red-sensitive photo-multiplier R 928 from Hamamatsu (www.hamamatsu.com). Measurements at 77 K were performed in a home-made cryostat cooled with liquid nitrogen. The emission spectra were corrected for the sensitivity of the PMT which was calibrated using a halogen lamp and 4-dimethylamino-4′-nitrostilbene [24,25].

Relative luminescence quantum yields were determined using a solution of PtOEP in toluene as a standard (Φ = 0.415 [26]). The solutions of the dyes were thoroughly deoxygenated by bubbling nitrogen through. The dyes were excited at 400 nm in the fluorescence spectrometer. The quantum yields also were determined

using a lock-in Amplifier (PreSens, www.presens.de) equipped with a silicon photo-diode. Excitation of PtOEP was performed with a 395 and a 405-nm LEDs (www.roithner-laser.com), while the benzoporphyrin complexes were excited with a 425 and 435-nm LEDs. A BG 12 filter (Schott, www.schott.com) was used for excitation and an OG 590 filter (Schott) for emission. The relative brightness of the LEDs was determined with a concentrated aqueous solution of 1-hydroxypyrene-3,6,8-trisulfonate in 0.1 M HCl used as a quantum counter.

Luminescence phase shifts for the dyes in solutions were measured with a two-phase lock-in amplifier (SR830, Stanford Research Inc., www.thinksrs.com). Excitation was performed with the light of a 435-nm LED (www.roithner-laser.com) which was sinusoidally modulated at frequencies of 6 and 1 kHz for the platinum(II) and palladium(II) complexes, respectively. A bifurcated fiber bundle was used to guide the excitation-light to the cuvette and to guide back the luminescence after passing the RG 9 (Schott) glass filter. The luminescence was detected with a photo-multiplier tube (H5701-02, Hamamatsu, www.sales.hamamatsu.com). Temperature was controlled by a cryostat ThermoHaake DC50. Gas calibration mixtures were obtained using a gas mixing device (MKS, www.mksinst.com).

Photo-bleaching experiments were performed using a lock-in amplifier from PreSens equipped with a photo-diode. The excitation was performed with the light of a 1 W 405-nm LED (www.roithner-laser.com) filtered through a BG 12 filter. An RG 630 filter (Schott) was used for the emission. A modulation frequency of 916 Hz was used. The concentration of dyes in poly(vinyl chloride) film was tuned so that similar luminescence intensities were obtained for all the indicators.

Cyclovoltammetric investigations were performed with the Autolab PGSTAT 100 potentiostat (Eco Chemie B.V., www.ecochemie.nl). The cell configuration was a three-electrode system consisted of platinum disc electrode as working electrode, platinum wire as counter electrode and a silver wire as pseudo-reference electrode. The electrolyte used in this measurements was a 5×10^{-4} M solution of the complexes in anhydrous dichlormethane (Roth) containing 0.1 M of tetrabutylammonium tetrafluoroborate ($TBABF_4$, Aldrich) as conducting salt. The cell was assembled and sealed under an argon atmosphere in a glovebox with a level of H_2O and oxygen <1 ppm. The scan rate for all measurements was 0.1 V s^{-1}. Ferrocene (Merck) was used as an internal standard and to reference the potentials against standard Ag/AgCl electrode ($E_{1/2}$ = 1.127 V [27]).

3. Results and discussion

3.1. Synthesis

The key steps of the synthesis of benzoporphyrin complexes include porphyrin ring formation according to the Lindsey method, metallation of the macrocycle and aromatization (Fig. 1). Since fluorinated derivatives can benefit from improved photo-stability and better solubility in polymers we have attempted to prepare the *meso*-substituted pentafluorophenylbenzoporphyrin complexes. Unfortunately, formation of the porphyrin macrocycle did not occur which is likely to be due to sterical reasons. However, less sterically ambitious mono-, di- and tri-fluorophenyl substituted cyclohexenoporphyrins can be obtained in good yields. It was also found that platination of the cyclohexenoporphyrins is promoted by the presence of the base so that the reaction time was reduced from 12 h [22] to tens of minutes. All the platinum(II) and palladium(II) complexes with cyclohexenoporphyrins are stable and can be isolated as individual substances. However, it was not always the case for the corresponding benzoporphyrin complexes. While the complexes with TPTBP and TPTBPF are stable, those formed by $TPTBPF_2$ and $TPTBPF_3$ cannot be isolated from the solution. Upon evaporation of the solvent (at air saturation or under nitrogen) decomposition to free-base porpyrin, metal and some other products occurs. The complexes however can be immobilized into polymers (such as polystyrene), where they are stable. If absorbed on silica-gel, they can be stored for months without noticeable decomposition and can be extracted into a solution for further use.

3.2. Photo-physical properties. Absorption

Fig. 2 illustrates spectral properties of platinum(II) benzoporphyrin complexes. The absorption spectrum consists of the Soret band located in the blue part of the spectrum and two Q-bands in the red part. It is interesting to compare spectral properties of the benzoporphyrin complexes with those of "classical" metalloporphyrins such as a platinum(II) complex with 5,10,15,20-tetrakis-(2,3,4,5,6-pentafluorophenyl)-porphyrin (PtTFPP) which is widely used in optical sensing. First, the Soret band of the respective benzoporphyrin complexes is bathochromically shifted by 40–45 nm compared to PtTFPP. Since the molar absorption coefficients for the Soret band exceed 200,000 M^{-1} cm^{-1}, extremely efficient excitation becomes possible. Cheap ultrabright 425 and 435 nm LEDs (10–20 mW) are available for the region and can be excitation sources of choice. Excitation in the blue region also is preferable over excitation in the UV because of much lower level of background fluorescence from the sample and optical components, and significantly higher transparence of cheap optical fibers to the excitation-light (if application in fiber-optic sensors is considered). Second, the benzoporphyrin complexes possess extremely efficient absorption in the red region, where molar absorption coefficients exceed 130,000 M^{-1} cm^{-1} (Table 1). For comparison, molar absorption coefficients of the "classical" porphyrins in the Q-bands typically are ~20,000 M^{-1} cm^{-1}. The efficient absorption in the red region makes the benzoporphyrin complexes potentially suitable for some important applications like measurements in straying turbid media or in subcutaneous tissue.

As can be seen from Fig. 2 and Table 1, substitution of hydrogen atoms to fluorine in the *meso*-positioned phenyl rings of the porphyrin results in a hypsochromic-shift of the Soret band and a bathochromic-shift of the Q-bands. The emission also shifts bathochromically. These effects may originate from the increased distortion of the porphyrin macrocycle [17]. Despite the fact that the red-shift of the Q-band is only minor (6 nm on going from

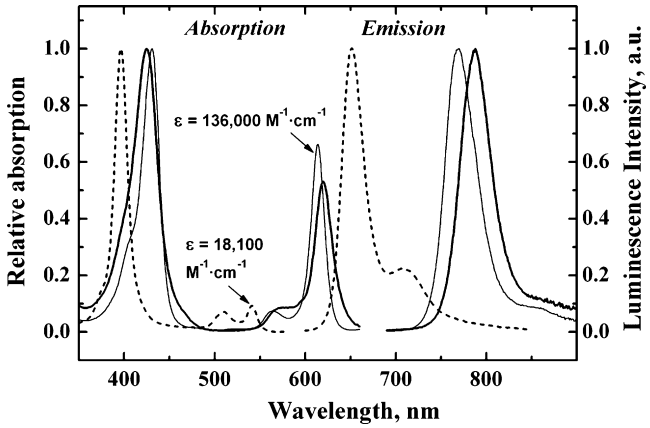

Fig. 2. Absorption and corrected emission spectra of PtTPTBP (thin lines), $PtTPTBPF_3$ (thick lines) and PtTFPP (dotted lines) in deoxygenated toluene at RT.

Table 1
Photo-physical properties of the platinum(II) and palladium(II) benzoporphyrin complexes in toluene.

Dye	λ_{max} abs (ε 10^{-3}), nm (M^{-1} cm^{-1})	λ_{max} em (nm)	Q.Y.	τ (μs)	λ_{max} em (77 K) (nm)	τ (77 K) (μs)	E_T[a], (cm^{-1})	k_q (Pa^{-1} s^{-1})
PtTPTBP	430 (205); 564 (16); 614 (136)	770	0.51	47	760	59	13160	102
PtTPTBPF	430 (212); 565 (16.3); 615 (146)	773	0.60	50	771	57	12970	95
$PtTPTBPF_2$	424 (1.00)[b]; 565(0.08); 617 (0.55)	786	0.37	46	778	55	12850	60
$PtTPTBPF_3$	424 (1.00)[b]; 569 (0.08); 620 (0.53)	788	0.27	38	782	51	12788	51
PdTPTBP	443 (416); 578 (21); 628 (173)	800	0.21	286	792	427	12630	60
PdTPTBPF	443 (268); 579 (12.7); 629 (115)	803	0.23	297	793	410	12610	59
$PdTPTBPF_2$	439 (1.00)[b]; 582 (0.065); 630 (0.27)	814	0.10	195	808	385	12380	63
PtTPTHPF	411 (245); 525 (18.8); 558 (24.4)	–	–	–	672	62	14880	–
PdTPTHPF	426 (234); 538 (22); 571 (19.5)	–	–	–	703	> 70	14220	–

[a] Calculated from the emission spectra at 77 K.
[b] Relative intensities.

PtTPTBP to $PtTPTBPF_3$, Table 1), it significantly improves compatibility of the porphyrins with the 632.8 nm of the He–Ne laser, but also 635 nm laser diode so that certain applications (for example in confocal microscopy) become possible. In fact, the molar absorption coefficient for PtTPTBP at 632 nm is only 11,200 M^{-1} cm^{-1}, but it becomes as high as ~24,000 M^{-1} cm^{-1} for $PtTPTBPF_2$ and ~48,000 M^{-1} cm^{-1} for $PtTPTBPF_3$. Since neither $PtTPTBPF_2$, nor $PtTPTBPF_3$ cannot be isolated as individual substances, these values were estimated based on the assumption that molar absorption coefficients in the Soret band for these dyes are similar to those of PtTPTBP and PtTPTBPF.

As expected, the absorption of respective palladium(II) complexes is bathocromically shifted by ~15 nm compared to the platinum(II) benzoporphyrins (Table 1). In the Soret band it peaks at 439–443 nm, and thus excitation by bright 450 nm LED is possible. The palladium(II) complexes can also be very efficiently excited by He–Ne laser and by red-emitting laser diodes.

3.3. Emission

All the benzoporphyrin complexes possess efficient phosphorescence in the NIR region (Fig. 2, Table 1). No fluorescence is detectable for the platinum(II) complexes and very little fluorescence (quantum yield, Q.Y. < 0.001) for the respective palladium(II) complexes. In case of PtTPTBP and PtTPTBPF the emission quantum yields are very high (0.5–0.6). For comparison, Q.Y. for PtOEP in toluene that was used as a standard is reported to be 0.415 [26]. As can be observed, fluorination of the phenyl ring results in a pronounced bathochromic-shift of the emission band. In case of platinum(II) and palladium(II) complexes with TPTBPF fluorination results in higher Q.Y. of luminescence and longer luminescence decay times τ. Further substitution (in 3 and 5 positions of the phenyl rings) results in significant decrease of both Q.Y. and τ, that is likely to originate from increased non-planarity of the molecule due to sterical effects. The complexes with *meso*-tetraphenyltetracyclohexenoporphyrins do not exhibit any detectable luminescence at RT and evidently are highly distorted. This is in a good agreement with the recent report of Vinogradov and co-workers [28]. These complexes, however, emit at 77 K (Fig. 3). At this temperature, the luminescence of palladium(II) porphyrins is much less intense than for the respective platinum(II) complexes that makes determination of the decay time difficult. In case of the benzoporphyrin complexes the trends observed at 77 K and at RT are similar (Table 1). However, the rigid character of the medium in the frozen glass evidently diminishes the distortion of the molecule so that the decrease in decay times on going from TPTBP to $TPTBPF_3$ is less pronounced. A similar trend is observed for RT luminescence of the complexes embedded into a rigid polymer matrix such as polystyrene. For example, the decay times in polystyrene measured at 25 °C are 55.3, 52.6, 52.0 and 45.7 μs respectively for PtTPTBP, PtTPTBPF, $PtTPTBPF_2$ and $PtTPTBPF_3$.

The low-temperature phosphorescence spectra allow more precise estimation of the energies of the triplet excited states (E_T). These values were extracted from the luminescence maxima and are summarized in Table 1.

The photo-physical properties of the benzoporphyrin complexes are summarized in Table 1. Among the benzoporphyrin complexes, PtTPTBPF has the best brightness (BS = ε Q.Y.) upon excitation in the Soret band (BS = 127,000) and in the Q-band (BS = 87,600). For comparison BS of the recently reported ultrabright iridium(III) coumarin complexes [13] is ~50,000, while for commonly used oxygen indicators PtTFPP and Ru-dpp BS is ~10,000 upon excitation in visible. Considering sensing applications, good BS results in high *S*/*N* and is especially important in case of thin sensor films and sensing nanobeads (that are preferably used in small concentrations to minimize interferences).

It is interesting to compare the photo-physical properties of the complexes with literature data available for PtTPTBP and PdTPTBP. Borek et al. [22] report ε = 203,000 M^{-1} cm^{-1} at λ_{max} = 430 nm and ε = 135,000 M^{-1} cm^{-1} at λ_{max} = 611 nm for PtTPTBP in an unspecified solvent, which is very close to our data. The emission (evidently for uncorrected spectra) is reported to peak at 765 nm at RT (τ = 53 μs) and at 751 nm at 77 K. Rogers et al. [17] report ε = 264,000 M^{-1} cm^{-1} at λ_{max} = 444 nm and ε = 105,000 M^{-1} cm^{-1} at λ_{max} = 629 nm for PdTPTBP in benzene. Our data indicate significantly higher molar absorption coefficients for PdTPTBP. Lower values obtained in case of PdTPTBPF may originate from small impurity of fine silica-gel present in the sample. The same authors

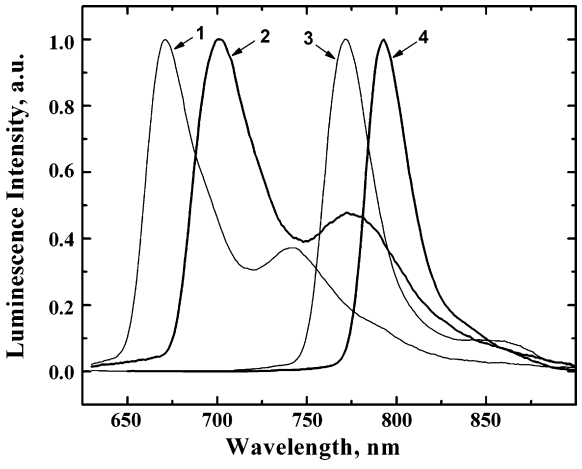

Fig. 3. Corrected emission spectra of platinum(II) and palladium(II) complexes at 77 K (toluene): (1) PtTPTHPF; (2) PdTPTHPF; (3), PtTPTBPF; (4) PdTPTBPF.

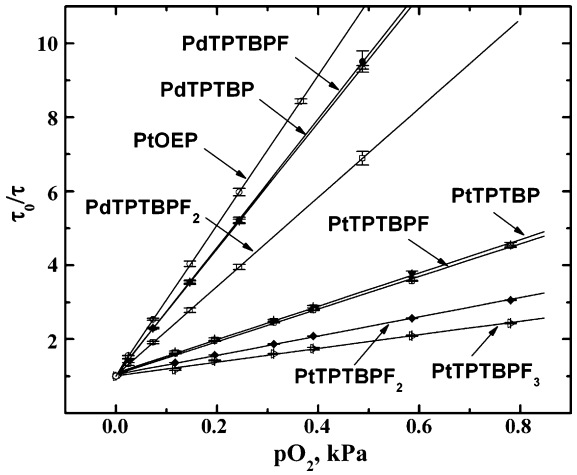

Fig. 4. Stern–Volmer plots for solutions of the benzoporphyrin complexes in toluene (~5×10^{-6} M, 25 °C).

report λ_{max} = 797 nm for the emission of PdTPTBP (Q.Y. = 0.17, τ = 195 μs) in pyridine.

3.4. Oxygen quenching

As was shown above all benzoporphyrin complexes possess long-lived phosphorescence that is effectively quenched by molecular oxygen. The Stern–Volmer plots obtained in toluene solutions are presented in Fig. 4 (τ_0 values are reported in Table 1). The quenching constants $k_q = K_{SV}/\tau_0$ calculated from the Stern–Volmer plots also are summarized in Table 1. Interestingly, for the benzoporphyrin complexes the quenching constants are not uniform and the following trend is observed: PtTPTBP > PtTPTBPF > $PtTPTBPF_2 \cong PdTPTBP \cong PdTPTBPF \cong PdTPTBPF_2 > PtTPTBPF_3$. The decrease in quenching efficiency roughly correlates with the decrease in energy of the triplet-excited state (Table 1). For comparison, in case of PtOEP (E_T = 15480 cm^{-1}) the quenching constant k_q was determined to be 210 $Pa^{-1}\,s^{-1}$ which is twice as high as the value obtained for PtTPTBP. To estimate the diffusion constant the Smoluchowski equation was used

$$k_d = 4\pi N_A 10^{-3}(D_{MP} + D_{O_2})(R_{MP} + R_{O_2}) \quad (1)$$

where D_{MP}, R_{MP}, D_{O_2} and R_{O_2} are diffusion coefficients and radii of the molecules of metalloporphyrine and oxygen, respectively; N_A, Avogadro's constant. For the calculation we used $R_{O_2} = 2 \times 10^{-8}$ cm [29] and $R_{MP} = 4.8 \times 10^{-8}$ cm [30]. D_{O_2} in toluene was assumed to be similar to that in benzene (5.7×10^{-5} $cm^2\,cm^{-1}$) [29]. D_{MP} in toluene was roughly estimated to be 1/10 of the $D_{O_2} = 5.7 \times 10^{-6}$ $cm^2\,cm^{-1}$ based on the data on diffusion coefficients available for solutions in acetonitrile and water (water: $D_{O_2} = 2 \times 10^{-5}$ $cm^2\,cm^{-1}$ [31] and $D_{MP} = 2 \times 10^{-6}$ $cm^2\,cm^{-1}$ [32,33]; acetonitrile $D_{O_2} = 7.12 \times 10^{-5}$ $cm^2\,cm^{-1}$ and $D_{MP} = 7.5 \times 10^{-6}$ $cm^2\,cm^{-1}$ [30]). The k_d was calculated to be 3.2×10^{10} $M^{-1}\,s^{-1}$, while the diffusion-controlled limit 1/9 k_d is calculated to be 3.6×10^9 $M^{-1}\,s^{-1}$. Considering that at 25 °C oxygen partial pressure of 1.013 10^5 Pa corresponds to the concentration of 9.06×10^{-3} M in toluene [34,35], the quenching constant for PtOEP is 210 $Pa^{-1}\,s^{-1} = 2.4 \times 10^9$ $M^{-1}\,s^{-1}$ that is rather close to the diffusion-controlled limit.

It is well known that quenching of the triplet excited state of a sensitizer by molecular oxygen occurs via energy transfer and results in the formation of singlet oxygen. Theoretical considerations [36] indicate that if the energy of the triplet state of an indicator is significantly higher than the energy of $^1\sum_g^+$ level of oxygen (E = 13121 cm^{-1} [36]) than energy is predominantly transferred to this state (Fig. 5a). In case of PtOEP the Gibbs energy of this process is very negative (−2360 cm^{-1}) and the process is diffusion-controlled. On the other side, the triplet energies of the benzoporphyrin complexes are very close to the energy of the $^1\sum_g^+$ level of oxygen (Table 1, Fig. 5a) so that the Gibbs energy is close to 0. In this case, the theory of energy transfer [37] predicts the dependence of quenching constant on the energy of triplet state of the sensitizers (Fig. 5b) while at rather negative Gibbs energies the process is expected to be diffusion controlled ($k_q \cong (1/9)k_d$). Indeed, the quenching constants for the benzoporphyrin complexes are significantly lower than for PtOEP and excellent correlation between E_T and k_q is observed in case of platinum(II) benzoporphyrins. The triplet energies of the palladium(II) benzoporphyrin complexes are already too low for the energy transfer to occur exclusively to $^1\sum_g^+$ state of oxygen. In this case, both the $^1\sum_g^+$ and $^1\Delta_g$ states are likely to be populated [36]. Further decrease in E_T of the sensitizer is likely to result in increase of the quenching constant since only the $^1\Delta_g$ state will be populated and the Gibbs energy of this process is very negative ($E(^1\Delta_g)$ = 7880 cm^{-1} [36]). It should be noted that other researchers obtained similar correlation between the quenching constant and the triplet energy of a photo-sensitizer in case of aromatic hydrocarbons [38] and water-soluble porphyrins [39,40].

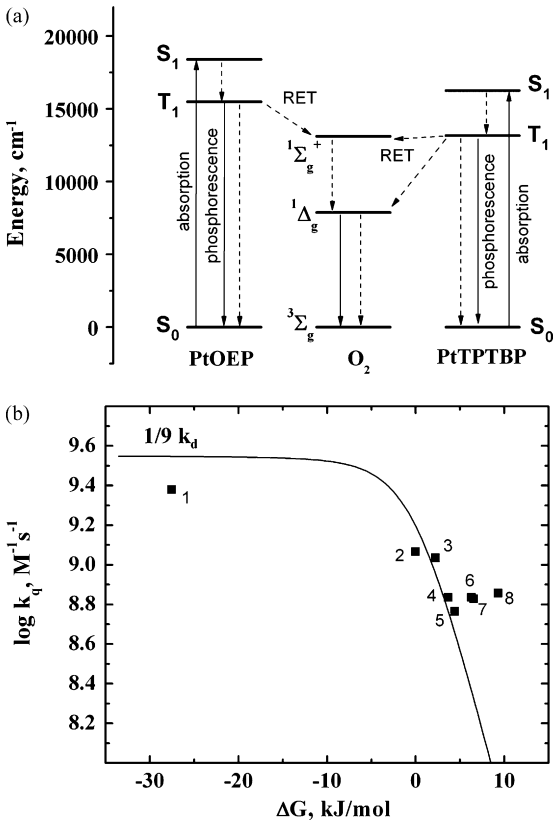

Fig. 5. (a) Jablonsky diagram for energy levels of PtOEP, PtTPTBP and molecular oxygen. Dashed arrows indicate radiationless processes and (b) dependence of the quenching constant on the free energy of the process $\Delta G = E\left(^1\sum_g^+\right) - E_T$. The squares indicate experimental data (1–8 is PtOEP, PtTPTBP, PtTPTBPF, $PtTPTBPF_2$, $PtTPTBPF_3$, PdTPTBP, PdTPTBPF, and $PdTPTBPF_2$) and the line is a fit using the equation from the theoretical model of the energy transfer [37].

Quenching of the porphyrin complexes (PtOEP, PtTPTBP, $PtTPTBPF_2$ and PdTPTBP) was also investigated in several polymers which significantly differ in polarity and rigidity. Very polar rigid poly(vinyl pyrrolidone) (PVP), polar rigid ethylcellulose (EC), apo-

Table 2
Quenching constants k_q ($Pa^{-1}\ s^{-1}$) and luminescence decay times τ (μs) of the porphyrin complexes in solution and in polymers (k_q/τ).

Complex	PtOEP	PtTPTBP	$PtTPTBPF_2$	PdTPTBP
Matrix				
Toluene	210/95	102/47	60/46	60/286
Chloroform	155/74	50/45	35/42	36/120
PVP	1.05/98	0.68/57	0.73/53	0.49/392
PS	3.49/71	3.07/55	3.46/52	3.01/356
EC	11.4/96	13.1/55	11.5/53	6.7/374
POMA	15.1/82	15.1/47	11.1/35	10.3/270

lar flexible poly(octadecyl methacrylate) (POMA) and apolar rigid polystyrene (PS) were chosen. The results are presented in Table 2. It should be mentioned that the Stern–Volmer plots obtained in the polymers are not linear and the fitting is performed using a "two-site" model [41]. As can be seen, for the solutions of dyes in chloroform the trend is similar to that observed in toluene. The situation is similar for the complexes embedded in PVP and to a less extent in POMA. When dissolved in EC, only PdTPTBP shows significantly lower quenching constant than other porphyrin complexes. Finally, in polystyrene all the complexes show similar quenching constants which may indicate that only the $^1\Delta_g$ level of oxygen is populated. The data presented in Table 2 also clearly indicate that the benzoporphyrin complexes are suitable as indicators for use in optical oxygen sensors. The sensitivity of the platinum(II) benzoporphyrin complexes is comparable to that of commonly used PtOEP. The palladium(II) complexes are more sensitive because of the longer luminescence decay times.

3.5. Photo-stability

This property is always of particular concern for practical applications especially in those cases where high-light densities are used or measurements are performed for prolong time. Photo-stability of the complexes was estimated upon continuous irradiation of the samples with 1 W LED and monitoring the emission intensity. We used poly(vinyl chloride) as a matrix since photo-bleaching is known to occur rather fast in this matrix but at the same time oxygen quenching is rather low. Data presented in Fig. 6 indicate that photo-stability of platinum(II) benzoporphyrin complexes is much higher than for PtOEP. In fact, after 50 min of irradiation ~3.5% of PtTPTBP is destroyed, compared to ~20% for PtOEP. As can be observed, photo-stability of PtTPTBPF is slightly higher (~3% photo-degradation in 50 min) than of PtTPTBP. This correlates well with the oxidation potentials obtained in electrochemical studies. For comparison, an extremely photo-stable PtTFPP [10] shows ~2% photo-degradation in the same condition. Photo-bleaching rates for the palladium complexes are significantly higher, which can originate from more effective oxygen quenching and consequently higher amount of singlet oxygen produced. We also observed a similar trend for photo-stability in case of the indicators embedded in polystyrene.

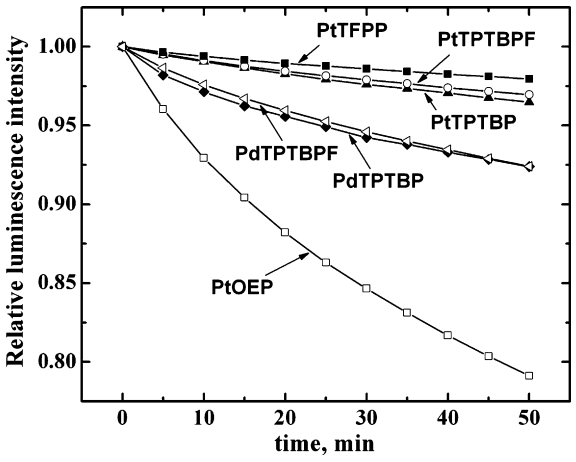

Fig. 6. Photo-degradation curves for the metalloporphyrins embedded in poly(vinyl chloride) films (~0.5% of an indicator, w/w; 2–7 μm thick films). Irradiation is performed with a 405-nm 1 W LED.

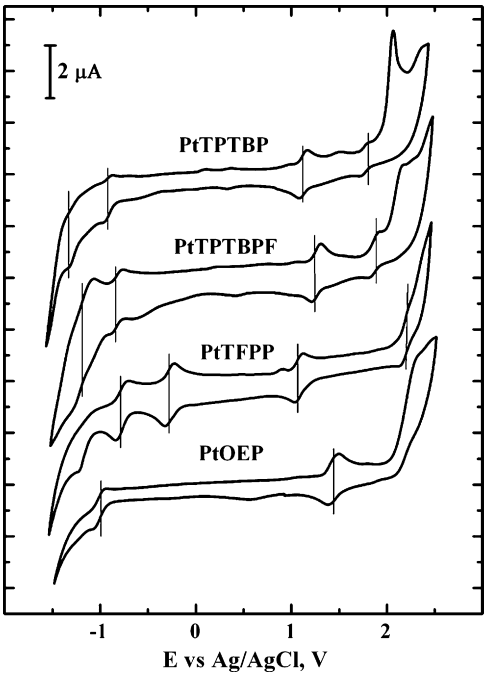

Fig. 7. Cyclic voltammograms of the platinum(II) porphyrin complexes ($C = 5 \times 10^{-4}$ M) in CH_2Cl_2 containing 0.1 M $TBABF_4$; scan rate 0.1 V s^{-1}.

Photo-degradation in most cases is due to singlet oxygen produced upon quenching that reacts with indicator molecules in the ground state to give products that are typically not luminescent. Therefore, we investigated the electrochemical properties of the new dyes. Cyclic voltammograms for two platinum(II) benzoporphyrin complexes PtTPTBP and PtTPTBPF are presented in Fig. 7. Cyclic voltammograms for PtTFPP and PtOEP also are shown for comparison. The half-wave potentials are compiled in Table 3. As can be observed, the oxidation and reduction potentials increase by ~0.1 V on going from TPTBP to TPTBPF complexes. Similar effects were observed by other researchers in case of fluorinated porphyrins [42]. Although this effect is minor, it still makes oxidation of the metalloporphyrins more difficult due to lower electron density. The increase in the oxidation potential correlates well with higher photo-stability of the TPTBPF complexes compared to the complexes of TPTBP. The reduction and oxidation potentials were

Table 3
Half-wave potentials (V vs. Ag/AgCl) of the benzoporphyrin complexes in CH_2Cl_2 containing 0.1 M $TBABF_4$ and scan rate 0.1 V s^{-1}.

Complex	Reduction		Oxidation	
	2nd	1st	1st	2nd
PtTPTBP	−1.27	−0.92	1.12	1.77
PtTPTBPF	−1.17	−0.82	1.26	1.87
PtTFPP	−0.77	−0.27	1.08	2.18
PtOEP	–	−1.01	1.44	1.44
PdTPTBP	−1.08	−0.73	1.27	1.84
PdTPTBPF	–	−0.70	1.38	1.88

found to be slightly higher for the palladium(II) benzoporphyrins than for the respective platinum(II) complexes. That is rather unexpected because electonegativity of palladium is lower than that of platinum. Unfortunately, it was not possible to estimate half-wave potentials for the $TPTBPF_2$ and $TPTBPF_3$ complexes, since they were found to be unstable in concentrated solutions during the electrochemical experiments.

4. Conclusions

Benzoporphyrin complexes with platinum(II) and palladium(II) represent promising alternatives to classical indicators for application in optical oxygen sensors. The complexes possess very high molar absorption coefficients in the blue region ($\varepsilon > 200{,}000\,M^{-1}\,cm^{-1}$) and in the red region ($\varepsilon > 130{,}000\,M^{-1}\,cm^{-1}$) and high emission quantum yields (>20%). Particularly the platinum(II) complexes show excellent brightnesses. Substitution of the hydrogen to fluorine in the *meso*-phenyl rings significantly improves the spectral compatibility of the platinum(II) complexes with the 632.8 nm line of He–Ne laser and 635 nm laser diode. In case of PtTPTBPF fluorination also improves luminescence quantum yields (to 60%) and photo-stability which is found to be comparable to that of PtTFPP. The quenching constants k_q for oxygen quenching in solutions are dependent on the energy of the triplet excited state E_T of the complexes. The quenching becomes less efficient with decreasing E_T which adequately agrees with the theory of energy transfer. The data obtained for the dyes dissolved in polymers indicate that all the complexes are promising as indicators for optical sensing of oxygen. Among them, $PtTPTBPF_2$, $PtTPTBPF_3$ and the palladium(II) complexes may be suitable for NIR confocal imaging of oxygen tension. PtTPTBPF is highly promising for other sensing applications because of its unmatched photo-physical properties.

Acknowledgement

This work was partly supported by the European Commission Sixth Framework program CLINICIP (EU 506965).

References

[1] O.S. Wolfbeis, J. Mater. Chem. 15 (2005) 2657–2669.
[2] Z. Rosenzweig, R. Kopelman, Anal. Chem. 67 (1995) 2650–2654.
[3] A. McEvoy, C. McDonagh, B.J. MacGraith, Sol–Gel Sci. Technol. 8 (1997) 1121–1125.
[4] P. Roche, R. Al-Jowder, R. Narayanaswamy, J. Young, P. Scully, Anal. Bioanal. Chem. 386 (2006) 1245–1257.
[5] A. Apostolidis, I. Klimant, D. Andrzejewski, O.S. Wolfbeis, J. Comb. Chem. 6 (2004) 325–331.
[6] V.D. Rumyantseva, N.P. Ivanovskaya, L.I. Konovalenko, S.V. Tsukanov, A.F. Mironov, N.S. Osin, Russ. J. Bioorg. Chem. 34 (2008) 239–244.
[7] D.V. Papkovsky, G.V. Ponomarev, W. Trettnak, P. O'Leary, Anal. Chem. 67 (2004) 4112–4117.
[8] A. Mills, A. Lepre, Anal. Chem. 69 (1997) 4653–4659.
[9] E.J. Park, K.R. Reid, W. Tang, R.T. Kennedy, R.J. Kopelman, Mater. Chem. 15 (2005) 2913–2919.
[10] S.K. Lee, I. Okura, Anal. Commun. 34 (1997) 185–188.
[11] Y. Amao, Y. Ishikawa, I. Okura, Anal. Chim. Acta 445 (2001) 177–182.
[12] M. DeRosa, P. Mosher, G. Yap, K. Foscaneanu, R. Crutchley, C. Evans, Inorg. Chem. 42 (2003) 4864–4872.
[13] S.M. Borisov, I. Klimant, Anal. Chem. 79 (2007) 7501–7509.
[14] S.M. Borisov, O.S. Wolfbeis, Chem. Rev. 108 (2008) 423–461.
[15] G. Khalil, M. Gouterman, S. Ching, C. Costin, L. Coyle, S. Gouin, E. Green, M. Sadilek, R. Wan, J. Yearyean, B. Zelelow, J. Porphyrins Phthalocyanines 6 (2002) 135–145.
[16] D.V. Papkovsky, G.V. Ponomarev, W. Trettnak, P. O'Leary, Anal. Chem. 67 (1995) 4112–4117.
[17] J.E. Rogers, K.A. Nguyen, D.C. Hufnagle, D.G. McLean, W. Su, K.M. Gossett, A.R. Burke, S.A. Vinogradov, R. Pachter, P.A. Fleitz, J. Phys. Chem. A 107 (2003) 11331–11339.
[18] O.S. Finikova, S.E. Aleshchenkov, R.P. Brinas, A.V. Cheprakov, P.J. Carroll, S.A. Vinogradov, J. Org. Chem. 70 (2005) 4617–4628.
[19] V.V. Rozhkov, M. Khajehpour, S.A. Vinogradov, Inorg. Chem. 42 (2003) 4253–4255.
[20] I. Dunphy, S.A. Vinogradov, D.F. Wilson, Anal. Biochem. 310 (2002) 191–198.
[21] T.J. Aartsma, M. Gouterman, C. Jochum, A.L. Kwiram, B.V. Pepich, L.D. Williams, J. Am. Chem. Soc. 104 (1982) 6278–6283.
[22] C. Borek, K. Hanson, P.I. Djurovich, M.E. Thompson, K. Aznavour, R. Bau, Y. Sun, S.R. Forrest, J. Brooks, L. Michalski, J. Brown, Angew. Chem. Int. Ed. 46 (2007) 1109–1112.
[23] O.S. Finikova, A.V. Cheprakov, I.P. Beletskaya, P.J. Carroll, S.A. Vinogradov, J. Org. Chem. 69 (2004) 522–535.
[24] R.J. Argauer, C.E. White, Anal. Chem. 36 (1964) 368–371.
[25] N.M. Emanuel, M.G. Kuzmin, Experimental Methods of Chemical Kinetics (in Russian), MGU, Moscow, 1985, pp. 152–157.
[26] A.K. Bansal, W. Holzer, A. Penzkofer, T. Tsuboi, Chem. Phys. 330 (2006) 118–129.
[27] N.G. Tsierkeros, J. Sol. Chem. 36 (2007) 289–302.
[28] A.Y. Lebedev, M.A. Filatov, A.V. Cheprakov, S.A. Vinogradov, J. Phys. Chem. A 112 (2008) 7723–7733.
[29] W. Ware, J. Phys. Chem. 66 (1962) 455–458.
[30] D. Kowalska, R.P. Steer, J. Photochem. Photobiol. A 195 (2008) 223–227.
[31] W.K. Subczynski, J.S. Hyde, Biophys. J. 45 (1984) 743–748.
[32] R.J.H. Chan, Y.O. Su, T. Kuwana, Inorg. Chem. 24 (1985) 3777–3784.
[33] P.A. Forshey, T. Kuwana, Inorg. Chem. 20 (1981) 693–700.
[34] P. Lühring, A. Schumpe, J. Chem. Eng. Data 34 (1989) 250–252.
[35] R. Battino, T.R. Rettich, T. Tominaga, J. Phys. Chem. Ref. Data 12 (1983) 163–178.
[36] D.R. Kearns, Chem. Rev. 71 (1971) 395–427.
[37] V. Balzani, F. Bolletta, F. Scandola, J. Am. Chem. Soc. 102 (1980) 2152–2163.
[38] A.A. Abdel-Shafi, D.R. Worrall, J. Photochem. Photobiol. A 172 (2005) 170–179.
[39] S.M. Borisov, V.V. Vasil'ev, Russ. J. Phys. Chem. 75 (2001) 1890–1895.
[40] V.V. Vasil'ev, S.M. Borisov, I.V. Golovina, Opt. Spectrosc. 95 (2003) 29–34.
[41] E.R. Carraway, J.N. Demas, B.A. DeGraff, J.R. Bacon, Anal. Chem. 63 (1991) 337–342.
[42] K.M. Kadisch, M. Lin, E. Van Caemelbecke, G. De Stefano, C.J. Medforth, D.J. Nurco, N.Y. Nelson, B. Krattinger, C.M. Muzzi, L. Jaquinod, Y. Xu, D.C. Shyr, K.M. Smith, J.A. Shelnutt, Inorg. Chem. 41 (2002) 6673–6687.